EUROPEAN LABORATORY FOR PARTICLE PHYSICS

ALEPH 2001-049
CONF 2001- 029
July 3, 2001

Study of B_s oscillations

PRELIMINARY

The ALEPH Collaboration

Abstract

This document contains two ALEPH Reports on three different analyses of B_s oscillations, based on the statistics collected by the ALEPH experiment during 1991-1995. B_s mesons are fully reconstructed in several hadronic decay channels, yielding a small sample of candidates with excellent decay length and momentum reconstruction. Semileptonic decays with a fully recontructed D_s meson yield larger statistics with equally high B_s purity, but somewhat degraded momentum resolution.
Inclusive semileptonic decays of b hadrons yield the highest sensitivity to B_s oscillations, due to the much higher statistics.

The combination of the above three with the other ALEPH analyses gives a limit of $\Delta m_{\rm s} > 10.7$ ps^{-1} at 95% C.L. with a sensitivity equal to 13.1 ps^{-1}.

Contributed Paper for LP01 and EPS HEP 2001

Study of B_s^0-$\overline{B_s}^0$ oscillations using fully reconstructed B_s^0 and $D_s^- - \ell$ events

PRELIMINARY

The ALEPH Collaboration

Abstract

A lower limit on the oscillation frequency Δm_s of the B_s^0-$\overline{B_s}^0$ system is obtained from recently reprocessed events taken with the ALEPH detector at LEP from 1991 to 1995. Fifty B_s^0 candidates with a purity of about 40% are fully reconstructed in the $D_s^- \pi^+$ and $D_s^- a_1^+$ decay modes in which the D_s^- decays into $\phi\pi^-$ or $K^{*0}K^-$. In addition, leptons are combined with fully reconstructed D_s^- candidates as evidence for B_s^0 decays, reconstructed in eight different decay modes, leading to 297 events. The initial state of the B_s^0 candidates has been determined using a neural network algorithm optimized to efficiently use the information of both sides of the event, with an average mistag rate of about 26%. The limit at 95% confidence level on Δm_s has been determined to be $\Delta m_s > 5.4$ ps^{-1}, with an expected sensitivity of 7.4 ps^{-1}.

Corresponding author: Fabrizio Palla (Fabrizio.Palla@cern.ch)

1 Introduction

The determination of the B_s^0 - $\overline{B_s}^0$ oscillation frequency Δm_s is one of the major issues in the study of flavour dynamics. So far, no experiment has yet directly observed B_s^0 oscillations, but a lower limit on Δm_s of 14.3 ps^{-1} has been set [1]. The present limit requires improvement of the proper time resolution of the oscillation analyses, since, in a simplified approximation, the damping of the oscillation effect coming from it has an exponential behaviour $\approx \exp(-\Delta m_s \sigma_t)$[2], where the σ_t is the error on the proper time. Fully reconstructed B_s^0 decays can help in the large Δm_s region, as already shown by DELPHI [3], due to their small proper time uncertainty with respect to other analyses.

During 1998 the LEP1 ALEPH data were reprocessed using a refined version of the reconstruction program. The main improvements concern track reconstruction and particle identification. A reanalysis of events containing a fully reconstructed D_s^- and a lepton has been performed, improving the selection efficiency by about 20%. A more powerful parametrization of the background and a better momentum error estimate allow substantial improvements at large Δm_s values compared to the old analysis [4, 5].

This paper presents the result of two analyses, one using $D_s^- - \ell$ events in which the D_s^- is completely reconstructed, and another, a new analysis, using exclusively reconstructed B_s^0 decays in totally hadronic final states. The full LEP1 statistics are used, which amount to about 4 million hadronic Z decays.

The paper is organized as follows. The next section deals with the $D_s^- - \ell$ events analysis, while Section 3 describes the fully reconstructed events analysis. Section 4 describes the tagging algorithm while in Section 5 the oscillation analysis and the systematic checks are discussed.

2 Reconstruction of $B_s^0 \to D_s^- \ell^+ \nu(X)$ decays

2.1 Event selection

In this section the selection of a sample of B_s^0 candidates in the $B_s^0 \to D_s^- \ell^+ \nu(X)$ decay channel, where the D_s^- is completely reconstructed, is presented.[1]

The D_s^- is reconstructed in six hadronic decay modes, $\phi\pi^-$, $K^{*0}K^-$, $K^-K_S^0$, $\phi\rho^-$, $K^{*0}K^{*-}$, $\phi\pi^+\pi^-\pi^-$, and two semileptonic modes, $\phi e^+\nu_e$ and $\phi\mu^+\nu_\mu$. The sources of background in the selected sample are: 1) $b \to D_s^- D_{(s)} X$ events, where $D_{(s)} \to \ell^+\nu(X)$; 2) kinematic reflections in the $K^{*0}K^-$ (K^-K^0) channel, from $D^- \to K^{*0}\pi^-$ ($K_S^0\pi^-$) decays; and 3) combinatorial background.

Cuts were optimized using about 8 million fully simulated $Z \to q\bar{q}$ events, 4 million $Z \to b\bar{b}$ events and samples of dedicated signal as well as background events.

The kaon identification requires a momentum of at least 1.5 GeV/c (to ensure a good kaon/pion dE/dx separation) and $\chi_\pi + \chi_K < 1$, where χ_H is the the difference between the measured and expected dE/dx ionization divided by its expected error. The pion identification requires $|\chi_\pi| < 3$ and a momentum larger than 0.5 GeV/c. The lepton identification is performed using standard criteria [7].

[1] Unless stated explicitly, charge conjugate states are implied.

The event selection proceeds similarly to the one described in [4, 5]. The invariant masses of the ϕ, K^{*0}, K^0_S, K^{*+} and ρ^+ mesons (being reconstructed respectively in the K^+K^-, $K^+\pi^-$, $\pi^+\pi^-$, $K^0_S\pi^+$ and $\pi^+\pi^0$ final states) must lie within $\pm$ 6, $\pm$ 50, $\pm$ 15 and $\pm$ 150 MeV/c^2 of their nominal mass. The lepton from the B^0_s is required to have a momentum larger than 2.5 GeV/c. The reconstructed D^-_s candidate is extrapolated back and vertexed together with the lepton to get the B^0_s decay vertex. The vertex probability associated to the D^-_s and to the B^0_s candidates must be at least 1%.

2.2 Sample composition

The results of the B^0_s selection on the data sample are summarized in Table 1. The D^-_s peak is fitted by two Gaussians for the signal (with widths and relative normalization taken from the simulation, and centered on the nominal value of the mass) and a second order polynomial for the background, fitted on $D_s\ell$ combinations with the wrong charge, if the statistics is reasonable, or on simulated events. For the leptonic modes a similar fit is performed to the ϕ mass peak. For the hadronic modes $K^{*0}K^-$, K^+K^0 and $K^{*0}K^{*-}$ a third Gaussian is included for the D^- peak. The mass spectra on data are shown in Fig. 1, together with the fit result.

In order to disentangle the contribution to the mass peak due to $b \to D_s{}^-D(X)$ events, the lepton momentum and transverse momentum, and the number of tracks forming a good vertex with the lepton, excluding the ones coming from the D^-_s, have been used to give an event-by-event estimate of the selection purity (Fig. 2). Typical values for the signal fraction in the resonant events are 85-95% if the transverse momentum is larger than 2 GeV/c, otherwise they are 65-80%, provided that the lepton momentum is larger than 15 GeV/c, or 35-80%, depending on the value of the number of vertexed tracks.

Channel	Efficiency (%)	Signal	$b \to D_sDX$	D^-	Combinatorial	Total
$\phi\pi^-$	12.1 ± 0.2	35.4	14.8	0	17.8	68
$K^{*0}K^-$	8.22 ± 0.17	38.4	14.5	15.0	45.1	113
K^+K^0	2.45 ± 0.08	9.8	3.7	0.7	9.8	24
$\phi\rho^-$	1.13 ± 0.08	6.2	1.4	0.6	13.8	22
$K^{*0}K^{*-}$	3.57 ± 0.16	7.4	3.0	0.4	8.2	19
$\phi\pi^+\pi^-\pi^-$	6.25 ± 0.27	3.6	1.3	0	8.1	13
$\phi e^-\overline{\nu}_e$	6.00 ± 0.30	7.6	2.3	0	9.1	19
$\phi\mu^-\overline{\nu}_\mu$	3.95 ± 0.24	9.7	3.8	0	5.5	19
Total		118.1	44.8	16.7	117.4	297

Table 1: Signal efficiency from Monte Carlo and estimated composition of the selected $D^-_s - \ell$ data sample; in the last column the number of candidates in the data for each channel is shown.

The experimental value of the total branching fraction for the $b \to D_sD(X)$ background is derived to be $BR(b \to D_sD(X))\cdot BR(D \to \ell X) = (1.3\pm0.3\pm0.4)\%$, while

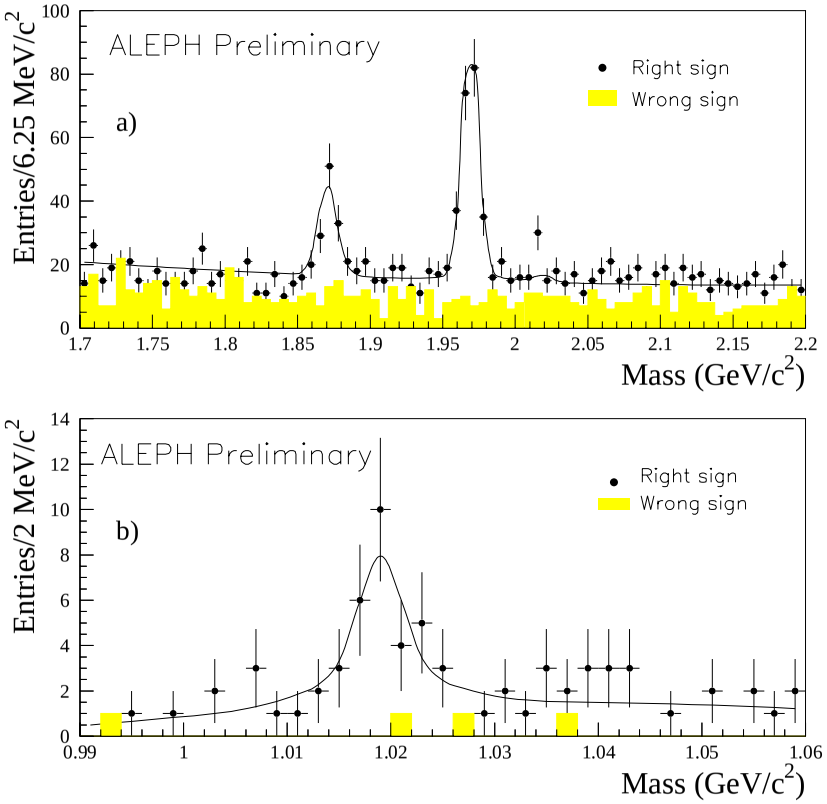

Figure 1: a) Mass spectra of the D_s^- candidates for the hadronic D_s^- decays and b) of the ϕ candidates for the semileptonic D_s^- decays, with the fit result. Mass spectra for $D_s^- - \ell$ combinations with the wrong charge correlation are also shown.

in the case of the signal the branching fraction is $BR(b \to B_s^0) \cdot BR(B_s \to D_s \ell \nu X) = (0.85 \pm 0.3)\%$ [8]. The ratio between the two branching fractions has been used to estimate the amount of $D_s D(X)$ events in the selected sample, taking into account the different selection efficiencies, and it has been varied by its error in the evaluation of systematic effects.

The relative fraction of B_d^0 in the background averaged over all channels amounts to about 40%.

2.3 Proper time measurement

The B_s^0 decay length l is measured by projecting the distance between the primary vertex and the B_s^0 vertex along the direction of the total momentum of the $D_s \ell$ pair. From Monte Carlo simulation, a negative bias on the decay length is determined to be of the order of -20 μm, and corrected for in the data. The decay length resolution is described by a Gaussian distribution, of width of 250 μm. The decay length error, as

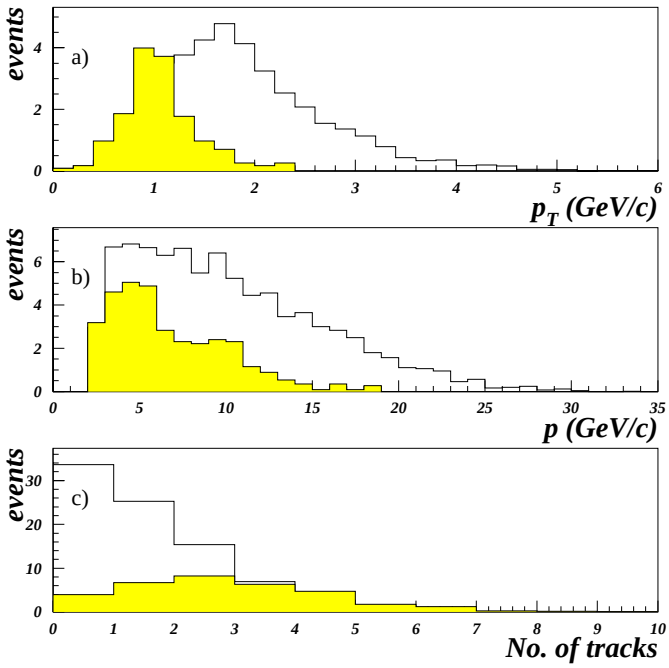

Figure 2: Discriminating variables in the Monte Carlo for the $b \to D_s D(X)$ background (shaded histogram) and the signal (white histogram): a) lepton transverse momentum, b) lepton momentum, c) number of tracks forming a good vertex with the lepton. The relative normalization is taking into account the selection efficiencies and the production rates.

evaluated from the track reconstruction algorithm, is found in the Monte Carlo to be underestimated by 10% on average, and is corrected accordingly in the data.

The decay length resolution in the data is found to be somewhat worse than suggested by the Monte Carlo simulation [**?**]. Therefore the decay length error is corrected for by 1.05 ± 0.03, for both the $D_s^- - \ell$ and fully reconstructed B_s^0 events.

The B_s^0 momentum, p, is estimated by using the neutrino energy, evaluated as the missing energy in the hemisphere:

$$E_\nu = E_{\rm tot}^{\rm hemi} - E_{\rm vis}^{\rm hemi} = E_{\rm beam} + \frac{m_{\rm same}^2 - m_{\rm oppo}^2}{4E_{\rm beam}} - E_{\rm vis}^{\rm hemi} \qquad (1)$$

where $m_{\rm same}$ and $m_{\rm oppo}$ are the invariant masses of the hemisphere containing and opposite to the B_s^0 respectively, and $E_{\rm vis}^{\rm hemi}$ is the visible energy in the hemisphere of the B_s^0 [6]. The bias on the measured momentum is corrected in the data, as a function of the momentum itself, using the formula

$$p_{\rm corr} = \frac{p}{1 + a + bp} \qquad (2)$$

where a and b are fitted in the Monte Carlo. The relative momentum error is parameterized as a linear function of the estimated momentum. Its average value is approximately 10%, with a core (20%) as good as 7%.

The proper time t is computed for each event as:

$$t = \frac{l}{\beta\gamma c} \tag{3}$$

where $\beta\gamma c$ is the boost of the $\mathrm{B_s^0}$. The error on the proper time is defined as :

$$\sigma_t = \sigma_l/(\beta\gamma c) \oplus \sigma_{\beta\gamma} \cdot t \tag{4}$$

where $\sigma_{\beta\gamma}$ is the relative momentum resolution. The predicted proper time distributions for the signal events have been obtained by convoluting their exponential functions with resolution functions evaluated from the simulated events, and can be written as:

$$\mathcal{R}(t_0, t) = \frac{1}{\sqrt{2\pi}\sigma_t} \exp\left(-\frac{(t-t_0)^2}{2\sigma_t^2}\right). \tag{5}$$

For the case of background events, both combinatorial and $\mathrm{D_sD}(X)$, the proper time distribution has been taken from the Monte Carlo simulation.

3 Reconstruction of hadronic $\mathrm{B_s^0}$ decays

The events are selected in the following decay modes:

$$\begin{array}{ll} \mathrm{B_s^0} \to \mathrm{D_s^{(*)-}}\pi^+(a_1^+) & ,\mathrm{D_s^-} \to \phi\pi^- \\ \mathrm{B_s^0} \to \mathrm{D_s^{(*)-}}\pi^+(a_1^+) & ,\mathrm{D_s^-} \to \mathrm{K^{*0}K^-} \end{array}$$

where the ϕ, $\mathrm{K^{*0}}$ and a_1 are reconstructed in their charged decay modes: $\phi \to \mathrm{K^+K^-}$, $\mathrm{K^{*0}} \to \mathrm{K^+}\pi^-$ and $a_1^+ \to \rho^0\pi^+$.

In order to reduce combinatorial background, all kaons and pions forming the $\mathrm{B_s^0}$ candidates must satisfy a cut $|\chi_h| < 3$.

3.1 Preselections of the $\mathrm{D_s^-}$ signal

For the reconstruction of $\mathrm{B_s^0} \to \mathrm{D_s^-}\pi^+$, all the track candidates are required to have a momentum greater than 1 GeV/c.

To reconstruct the neutral daughter of the $\mathrm{D_s^-}$ ($\phi \to \mathrm{K^+K^-}$, $\mathrm{K^{*0}} \to \mathrm{K^+}\pi^-$), pairs of oppositely charged tracks inside a cone of 90^o are required to have an invariant mass consistent with the nominal mass of a ϕ or $\mathrm{K^{*0}}$. A third track is then combined with each of these pairs to form a three-prong $\mathrm{D_s^-}$ vertex. Candidate tracks are first fitted to a common vertex. If the mass of the vertex is within ± 30 MeV/c^2 of the $\mathrm{D_s^-}$ nominal mass, the vertex is refitted with the $\mathrm{D_s^-}$ mass constraint. The χ^2-probability of the $\mathrm{D_s^-}$ vertex is required to be greater than 1%. The reconstructed ϕ, $\mathrm{K^{*0}}$ and $\mathrm{D_s^-}$ mesons must have a momentum greater than 3 GeV/c. The decay of the pseudoscalar meson $\mathrm{D_s^-}$ into a vector meson (ϕ or $\mathrm{K^{*0}}$) and a pseudoscalar meson (π^-) follows a distribution

proportional to $\cos^2\lambda$, where λ is the helicity angle defined as the angle between the π^- (K^-) from D_s^- and one of the $\phi(K^{*0})$ daughters in the $\phi(K^{*0})$ rest frame. To reduce the combinatorial background, we require $|\cos\lambda| > 0.4$.

The D_s^- candidate is further combined with a remaining π candidate in the same event to form a B_s^0 vertex. The D_s^- vertex has to be in front of the B_s^0 vertex. All the B_s^0 candidates are then subject to the final cuts, discussed in the Section 3.3.

The event preselection efficiency in the $\phi\pi$ channel is 35% and 25% for the $K^{*0}K^-$ channel.

3.2 Preselection of the a_1^+ signal

To reconstruct the D_s^- for $B_s^0 \to D_s^- a_1^+$, all the preselection cuts are the same as for the channel $B_s^0 \to D_s^-\pi^+$.

For reconstructing $a_1^+ \to \rho\pi^+ \to \pi^-\pi^+\pi^+$, the momentum of the pion candidates are required to be greater than 0.5 GeV/c and the momentum of the reconstructed ρ and a_1 to be greater than 1 GeV/c. Three pion candidates, two of which have an invariant mass within ± 150 MeV/c^2 of the ρ nominal mass, are required to form a common vertex with the χ^2-probability of the vertex fit greater than 1%. The difference between the invariant mass and the mass of a_1 should be within the natural width of the a_1 (± 300 MeV/c^2).

The efficiency of the event selection is 24% for $\phi\pi$ and 26% for $K^{*0}K^-$ channel.

3.3 Final cuts and event selection efficiencies

Selected D_s^- candidates are combined with a π^+ candidate or an a_1^+ candidate to form a B_s^0 vertex with the vertex fit probability greater than 1%. To be sure that the B_s^0 flight path is along the B_s^0 momentum direction, $cos(\alpha) \geq 0.97$ is required, where α is the angle between the B_s^0 decay length direction and the B_s^0 momentum. The B_s^0 vertex is required to be well displaced from the primary vertex to cut combinatorial background, i.e. B_s^0 decay length significance $l_{B_s}/\sigma_l > 3$, where l_{B_s} is the B_s^0 decay length and σ_l the error of the decay length. This cut alone has a 80% efficiency for the signal events.

The B_s^0 momentum is required to be larger than 20 GeV/c for the $D_s^-\pi^+$ channel, while for the $B_s^0 \to D_s^- a_1^+$ channel the momentum cut to is increased to 30 GeV/c. If more than one combination is present per event, only the one with the highest B_s^0 momentum has been kept.

The average reconstructed B_s^0 mass resolution in the different decay modes ranges from 17 to 25 MeV/c^2.

Candidate events whose mass fall within ± 75 MeV/c^2 of the B_s^0 mass are selected.

Events in which the B_s^0 decays into a D_s^{*-} have a lower reconstructed invariant mass, because of the undetected photon. From the Monte Carlo simulation they are predicted to populate the region between 5 and 5.3 GeV/c^2 (referred in the following as satellite peak).

The event selection efficiencies for the different channels range from 6 to 21 % and are shown in Table 2:

Channel	Efficiency (%)
$B_s^0 \to D_s^- \pi^+ (\phi\pi^-)$	21 ± 1
$B_s^0 \to D_s^- \pi^+ (K^{*0}K^-)$	16 ± 1
$B_s^0 \to D_s^- a_1^+ (\phi\pi^-)$	11 ± 1
$B_s^0 \to D_s^- a_1^+ (K^{*0}K^-)$	6 ± 1

Table 2: Event selection efficiencies for each channel.

3.4 Sample composition

Figure 3 shows the B_s^0 mass spectra for the $D_s^- \pi^+$, $D_s^- a_1^+$ and the sum of the two channels using data collected from 1991 to 1995, after all the selection criteria described in the previous section. The data are indicated by points and error bars. The narrow peak at 5.37 GeV/c^2 clearly indicates the signal events in this channel. The broader shoulder structure peaked at around 5.1 GeV/c^2 is due to the events of the type $B_s \to D_s^{*-} \pi^+$ with $D_s^{*-} \to D_s^- \gamma$, where the cascade photon has not been reconstructed. The data are in good agreement with the Monte Carlo prediction.

Figure 4 shows instead the mass spectrum of the D_s^- sideband events in the data. The signal events in the data are also superimposed.

The purity of the signal and the composition of the background can be evaluated from the Monte Carlo samples and are reported in Table 3. In the Δm_s fit, the purity and the background composition have been taken from the simulation.

Region	B_s^0 purity (%)	B_d^0 fraction of the background (%)
Main peak $D_s^- \pi^+$	64 ± 9	44 ± 16
Satellite peak $D_s^- \pi^+$	43 ± 7	58 ± 12
Main peak $D_s^- a_1^+$	30 ± 6	47 ± 12
Satellite peak $D_s^- a_1^+$	30 ± 8	54 ± 10

Table 3: Fraction of background in the two mass peak regions for the two decay channels predicted from the Monte Carlo simulation.

The background is coming almost entirely from $b\bar{b}$ events, in which the D_s^- can either be a true one or not. In the $D_s^- a_1^+$ channel, due to the broad a_1^+ mass window cut, the main part of the combinatorics is coming from decays of the b-hadron in which some of the pions are falling inside the desired mass region. Out of 9 million Monte Carlo b-hadron decays, the fraction of B_s^0 decays is predicted to be less than 2% of the total background for the $D_s^- \pi^+$ channel and about 9% in the case of $D_s^- a_1^+$. Some of the most important branching ratios for hadronic decays of the b-hadrons in the Monte Carlo simulation are given in Table 4.

In the $D_s^- \pi^+$ channel the main source of non-B_s^0 decays are D^- reflections: $B_d^0 \to D^- \pi^+$. The Monte Carlo predicts that this source mainly affects the $K^{*0}K^-$ channel, since the K^{*0} resonance is broader than the ϕ and a $D^- \to K^{*0}\pi^-$ decay can fake a

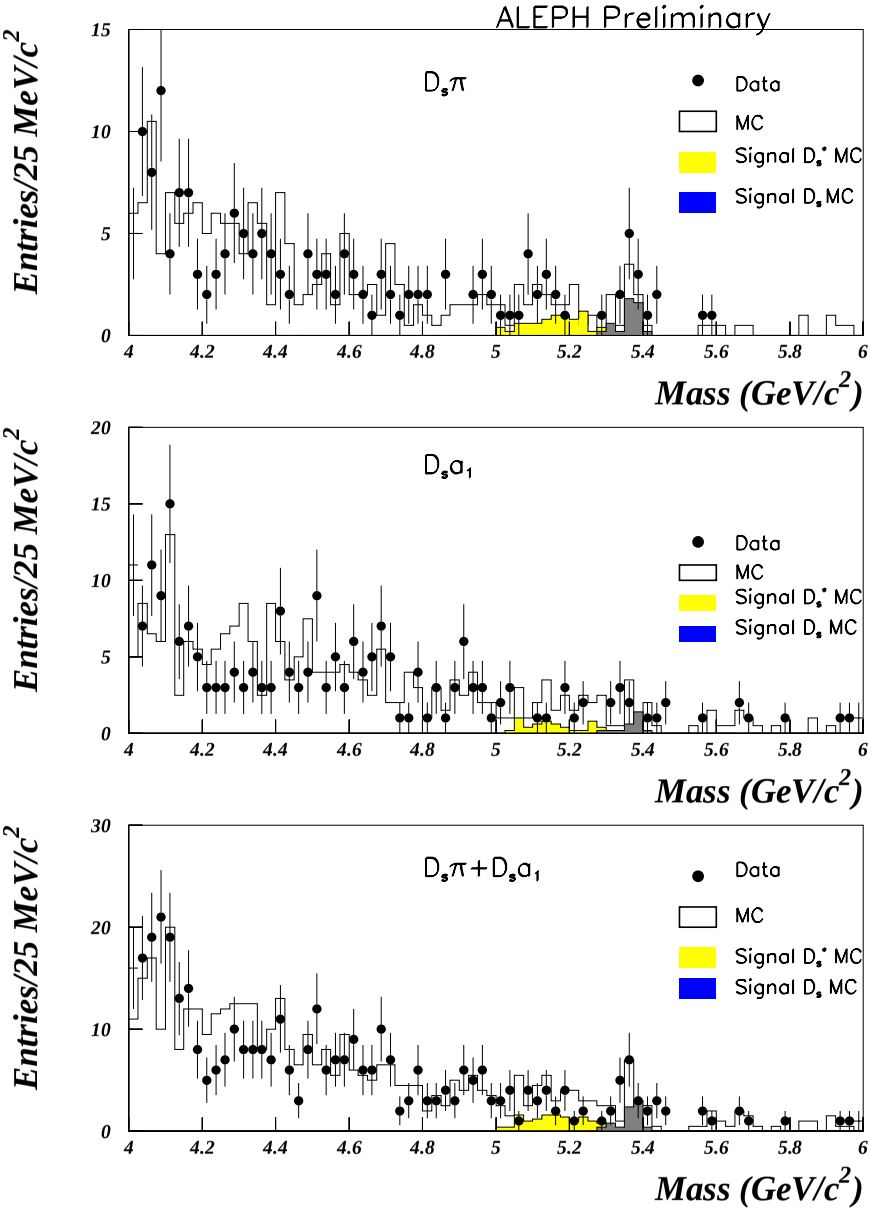

Figure 3: The mass spectrum of the $D_s^- \pi^+$ and $D_s^- a_1^+$ candidates. The points and error bars are the data, the histograms are the Monte Carlo. The dark shaded histograms show the contribution of the signal decays into $D_s^- \pi^+$ and $D_s^- a_1^+$. The light shaded histograms show the contribution of the signal decays into $D_s^{*-} \pi^+$ and $D_s^{*-} a_1^+$. The first plot refers to the $D_s^- \pi^+$ channel, the second to the $D_s^- a_1^+$ channel, while the last one is the sum of the first two.

$D_s^- \to K^{*0} K^-$ decay if the π^- is misidentified as a K^-. Within ± 75 MeV/c^2 of the B_s^0 mass, 11 events remain in the mass peak out of 1300 generated Monte Carlo samples

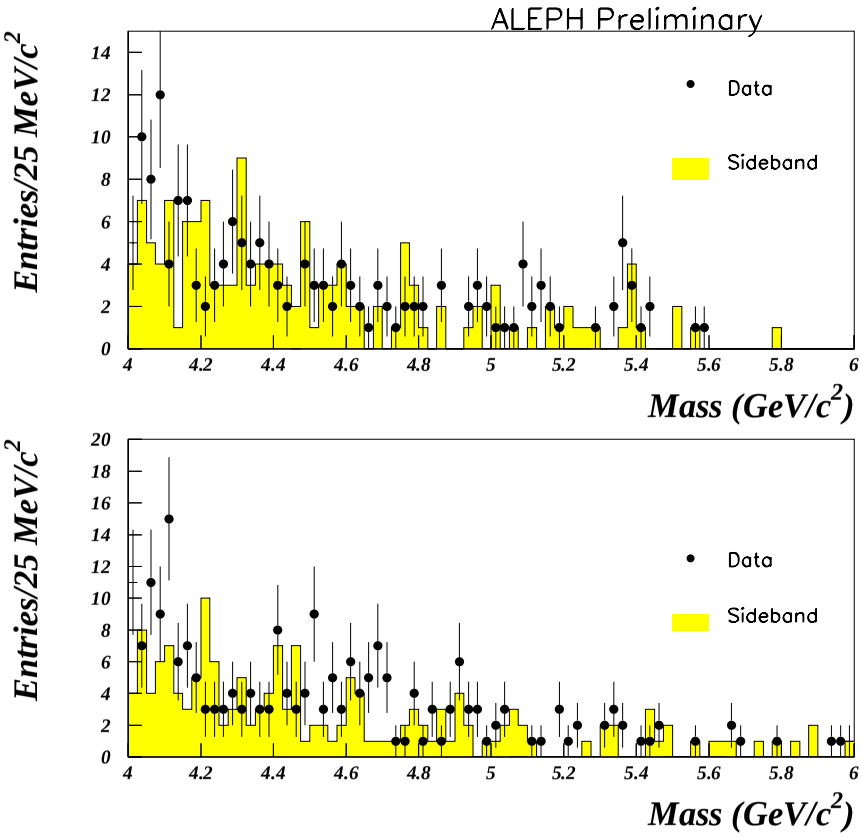

Figure 4: The mass spectrum of the D_s^- side bands candidates in the data for the $D_s^-\pi^+$ (upper plot) and $D_s^- a_1^+$ (lower plot) decay modes, together with the good combinations shown as points and error bars.

of B_d^0 events having passed through the full reconstruction algorithms and satisfying the selection criteria. Assuming the branching ratios: $BR(B_d^0 \to D^-\pi^+) = (3.0 \pm 0.4) \times 10^{-3}$, $BR(D^- \to K^-\pi^-\pi^+) = (9.0 \pm 0.6)\%$, one expects 1.5 ± 0.2 B_d^0 events in the $B_s^0 \to D_s^-\pi^+$, $D_s^- \to K^{*0}K^-$ channel [8].

After the selection, looking into the region of $\pm$ 75 MeV/c^2 of the B_s^0 mass, there are 12 events reconstructed in the $D_s^-\pi^+$ channel and 9 in the $D_s^- a_1^+$. There are additional 16 and 13 events that can be recuperated from the D_s^* satellite peaks in the two decay modes, respectively.

The total number of signal events is estimated to be 10$\pm$3 in the main peak and 9$\pm$4 in the satellite peak.

3.5 Proper time measurement

The decay length is calculated as the distance between the B_s^0 vertex and the primary vertex projected on the direction of the B_s^0 momentum. Monte Carlo study shows

Decay mode	Branching Ratio(%)
$B_s^0 \to D_s^{*-}\pi^+$	0.284
$B_s^0 \to D_s^{*-}a_1^+$	0.764
$B_d^0 \to D^-\pi^+$	0.262
$B_d^0 \to D^-a_1^+$	0.677
$B^+ \to D^{*0}\pi^+$	0.64
$B^+ \to D^{*0}\rho^+$	1.49
$B^+ \to D^{*0}a_1^+$	1.49

Table 4: Values of the branching ratios for the some of the hadronic decay modes in the Monte Carlo simulation.

that B_s^0 decay length resolution is about 150 μm, while the momentum resolution for events in the main peak is of the order of 0.5% giving a proper time resolution of about 0.08 ps. Events with undetected photon coming from the D_s^{*-} have a good boost resolution as well (about 3%), due to the fact that the missing photon energy cancels in the ratio of the satellite B_s^0 momentum and mass. The pull of the decay length distribution for fully reconstructed events can be fitted with two Gaussian functions of widths $\sigma_1 = 1.03 \pm 0.03$ and $\sigma_2 = 2.1 \pm 0.8$, where the broader Gaussian accounts for 5% of the total only. For events in the satellite peak the width is consistent with a single Gaussian of $\sigma = 1.08 \pm 0.06$. In the fit to Δm_s the decay length error is evaluated on an event by event basis, and corrected by the pull width as predicted from the Monte Carlo simulation.

Except for the combinatorial background contribution, the predicted proper time distributions for the signal and B_d^0 events have been obtained by convoluting their exponential functions with resolution functions evaluated from the simulated events. The combinatorial background under the peak has been parametrized as $t/\tau^2 \exp -t/\tau$ with $\tau = 0.56 \pm 0.07$ ps, as predicted from the simulation.

4 Tagging

For each candidate event a combined mistag rate η is then defined as

$$\eta = \eta_I(1 - \eta_f) + \eta_f(1 - \eta_I) \tag{6}$$

using the initial state and final state mistag probabilities η_I and η_f respectively.

4.1 Final state tag

The flavour state of the decaying B_s^0 is estimated from the charge of the reconstructed D_s^-. Signal events are always correctly tagged. Events where the D_s^- are produced via a W have always the wrong tag, while in a generic background event, the mistag can vary depending on its real nature. The final state mistag η_f has been evaluated using the Monte Carlo simulation.

4.2 Initial state tag

The flavour state at production time is estimated using two sets of discriminating variables which are combined into a single tag variable. Firstly, in the hemisphere opposite to the B_s^0 candidate a neural network is applied, which is then combined with five discriminating variables computed using charged tracks in the same side as the B_s^0 candidate.

Opposite hemisphere tag The initial-state tag on the side of the event opposite to the fully reconstructed B_s candidate is performed using a neural network to combine a sequence of charge estimators. The input charge estimators to this network are :

1. *Jet charges*, Q_κ, are formed in the usual way [9] using three different values of the weighting power, κ: 0.5, 1.1 and 2.2. These focus on correspondingly higher values of track momenta and are highly correlated.

2. *The secondary vertex charge*, $Q_{\rm vtx}$, is formed using the output from a track separation neural network according to : $Q_{\rm vtx} = \sum_{i=\rm tracks} w_i\, q_i$ where q_i and w_i are respectively the charge of the tracks and the output of a dedicated neural network used to separate fragmentation and b-hadron tracks respectively.

3. *The momentum weighted primary vertex charge*, $Q_{\rm Pvtx}$, is calculated with the aim of achieving a reasonable initial state mistag for B^0 hemispheres. It is calculated according to : $Q_{\rm Pvtx} = \sum_{i=\rm tracks}(1-w_i)\, q_i\, p_{\rm L}^i / \sum_{i=\rm tracks} p_{\rm L}^i$.

4. *The momentum weighted secondary vertex charge*, $Q_{\rm Svtx}$, is calculated in an analogous manner according to : $Q_{\rm Svtx} = \sum_{i=\rm tracks} w_i\, q_i\, p_{\rm L}^i / \sum_{i=\rm tracks} p_{\rm L}^i$ but with the aim of improving the mistag for both charged and neutral B decays *via* leading particle effects from the secondary decay.

5. *In semileptonic B decays* the lepton momentum and transverse momentum are used as they contain information on the probability that the charge of the lepton candidate be the same as the charge of the b quark from the Z decay.

6. *Fast kaon identification* is used from a further dedicated neural network trained to identify kaons coming from b-hadron decays. The neural network uses the dE/dx information from the TPC and the track separation neural network w_i as inputs. In the bulk of events, there is only one true kaon from the b-hadron decay per hemisphere. Hence, a single charged track with the maximal value of the fast kaon neural network output is selected and this maximum value is then signed with the track charge.

In addition to the above charge estimators, three control variables are used, in order to provide the initial-state neural network with information regarding the overall topology of the b-hadron decay, and the quality of information present in a given hemisphere :

1. *The reconstructed b-hadron momentum* is supplied to provide information on the relative momenta of tracks coming from the primary and secondary vertices.

2. *The reconstructed proper time of the b-hadron* is based on the reconstructed b-hadron momentum and the measured decay length. The intention here is to incorporate the increased probability of $B^0_{\rm d}$ mixing at long proper times.

3. *The spread of the track separation weights*, $\sigma = \sum_{i=\rm tracks} w_i\,(1-w_i)$ which are used in several of the charge estimators. This allows to deweight those charge estimators which are dependent on a clear allocation of tracks to the primary and secondary vertices in cases of high charged multiplicities and/or poor vertexing.

Same hemisphere tag For the same side of the reconstructed $\rm B^0_s$ one profits of the fact that all the tracks coming from the $\rm B^0_s$ have been already selected. Therefore an effort to identify fragmentation tracks from the fragmentation process that leads to the $\rm B^0_s$ hadron has been performed. Firstly a jet containing the $\rm B^0_s$ tracks is found using a $y_{cut} = 0.02$ with the JADE algorithm. Using the charged tracks within that jet that do not belong to the $\rm B^0_s$, five discriminating variables are defined, together with the reconstructed momentum of the $\rm B^0_s$:

- three jet charges with $\kappa = 0, 0.5$ and 1;
- the $q \cdot p_L$ of the best kaon candidate that has an impact parameter significance with respect to the primary vertex smaller than 5, where q is the kaon charge and p_L its longitudinal momentum with respect to the $\rm B^0_s$. If more than one kaon is found, then the one with the best χ_K is taken;
- the dE/dx estimator χ_K of the above best kaon candidate.

4.3 Combined tag performance

Figure 5 shows the distribution of the final discriminating variable for initially produced $\rm B^0_s$ and $\overline{\rm B_s}^0$, in the Monte Carlo simulation. The probability η_I to tag incorrectly the initial state is evaluated for each value of the tag using dedicated samples of Monte Carlo events, both for the signal and the physical backgrounds. The average effective mistag for the signal is about 26% for both the fully reconstructed and $\rm D^-_s - \ell$ events.

5 Oscillation analysis

A $\rm B^0_s$ candidate is tagged as unmixed (mixed) when the reconstructed initial and final flavour states are the same (opposite) and they are labelled in the following with ss (os)

The oscillation analysis is performed using the amplitude method [2], which consists of measuring, for each $\Delta m_{\rm s}$ value of the oscillation frequency, an amplitude $\mathcal{A}$ and its error $\sigma_{\mathcal{A}}$. The $\mathcal{A}$ parameter represents the amplitude of the oscillatory part of the time evolution for a mixed or unmixed $\rm B^0_s$ state:

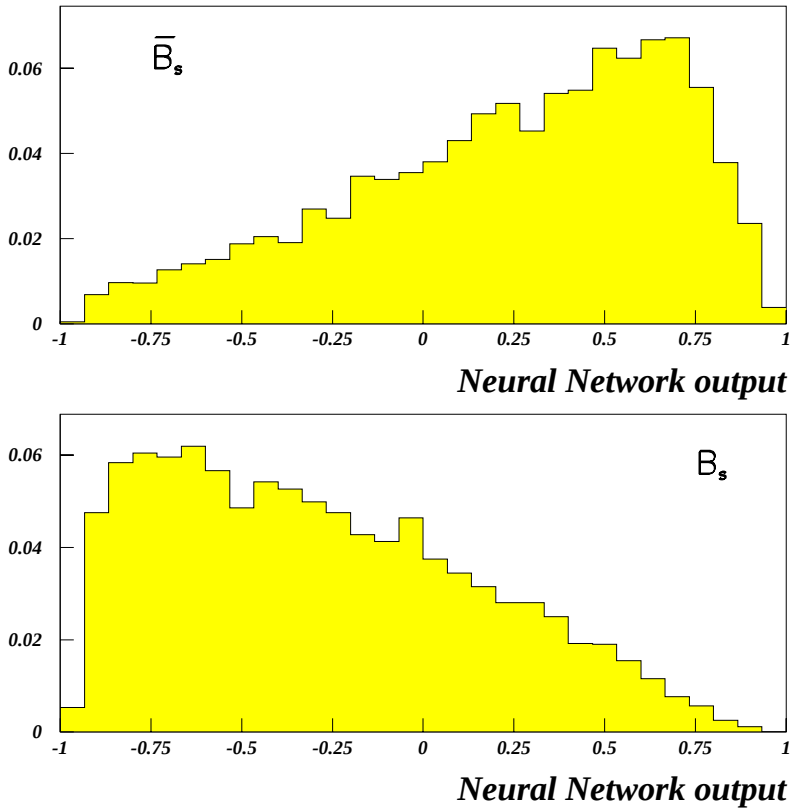

Figure 5: Final neural net output variable for initially produced $\overline{\mathrm{B_s}}^0$ and $\mathrm{B_s^0}$ states.

$$\mathcal{P}_s^{mix,unmix}(t) = \frac{1}{2\tau_s} \exp\left(-t/\tau_s\right) \left(1 \mp \mathcal{A} \cos(\Delta m_{\mathrm{s}} t)\right). \tag{7}$$

The 95% CL lower limit for Δm_{s} is obtained evaluating the probability that a real signal having an amplitude equal to unity would give an observed amplitude smaller than the one measured, in at most 5% of the cases. This corresponds to the condition $\mathcal{A}(\Delta m_{\mathrm{s}}) + 1.645\sigma_{\mathcal{A}}(\Delta m_{\mathrm{s}}) < 1$.

A likelihood function can be written for events tagged as mixed and unmixed:

$$\mathcal{L} = \prod_i^{\mathrm{ss}} F^{ss}(t_i) \prod_i^{\mathrm{os}} F^{os}(t_i). \tag{8}$$

For each of the mixed or unmixed tagged event a probability density function can be written as:

$$F^{os}(t_i) = f_{sig} F_s^{os}(t_i) + (1 - f_{sig}) \left(f_d F_d^{os}(t_i) + (1 - f_d) \eta_b F_{bkg}^{os}(t_i) \right) \tag{9}$$

where f_{sig} is the signal fraction, f_d is the fraction of B_d^0 in the background, and have been evaluated as explained in Sections 3.4 and 2.2. The expressions for the different probability density functions are given by:

1. for the B_s^0 tagged as mixed events:

$$F_{sig}^{os}(t_i) = \left[(1-\eta_s)\mathcal{P}_s^{mix}(t) + \eta_s \mathcal{P}_s^{unmix}(t)\right] \otimes \mathcal{R}_s(t-t_i) \tag{10}$$

2. for the B_d^0 tagged as mixed events in the exclusive analysis:

$$F_d^{os}(t_i) = \left[(1-\eta_d)\mathcal{P}_d^{mix}(t) + \eta_d \mathcal{P}_d^{unmix}(t)\right] \otimes \mathcal{R}_d(t-t_i) \tag{11}$$

3. in the case of the $D_s^- - \ell$ analysis the B_d^0 probability density function has been parametrized using the Monte Carlo simulation, as explained in Section 2.3.

The expressions for the events tagged as unmixed $F^{ss}(t_i)$ are described by changing η with $1-\eta$. The probability density functions $F_{bkg}(t_i)$ for the remaining background have been parametrized as explained in Sections 2.3 and 3.5.

5.1 Systematic uncertainties

Uncertainties in the evaluation of the input parameters in the fit have been propagated and the corresponding variation in the fitted amplitude has been taken as the systematic error.

- Variations in the fractions of signal and background events have been varied within their statistical errors, as given in Sections 2.2 and 3.4.
- The systematic error from the decay length is evaluated by scaling the resolution in decay length by ± 0.03 as explained in Section 2.3. For momentum the systematic error has been evaluated propagating the statistical errors in the Monte Carlo.
- A 10% relative error on the initial state mistag is taken as a correlated systematic error for both exclusive and $D_s^- - \ell$ events.
- The B_s^0 lifetime and Δm_d have been varied within errors taken from [8], while errors in the the parametrization of the background proper time have been taken into account as explained in Sections 2.3 and 3.5.

5.2 Limit on Δm_s

An unbinned likelihood fit is performed firstly to the $D_s^- - \ell$ events alone. Fig. 6 shows the result of the fit to the amplitude as a function of Δm_s. A limit at 95% CL has been obtained

$$\Delta m_s > 5.2 \text{ ps}^{-1} \text{ at } 95\% \text{ CL} \tag{12}$$

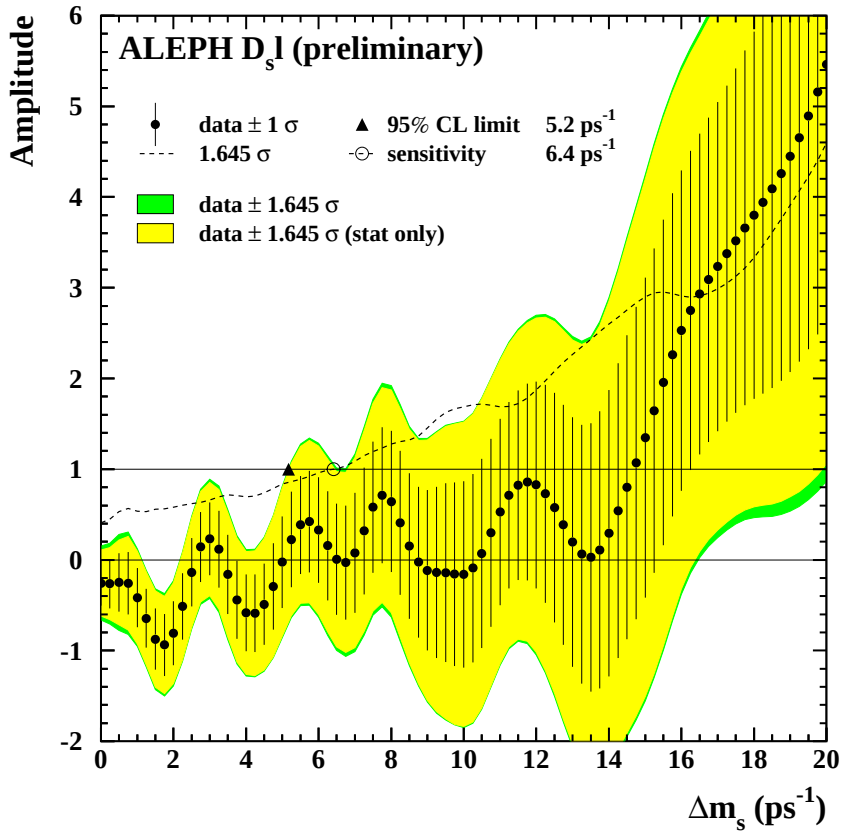

Figure 6: Measured amplitude as a function of $\Delta m_{\rm s}$ for the $\rm D_s^- - \ell$ events alone. The error bars represent the 1σ statistical uncertainties and the shaded bands show the one-sided 95% CL contour, with and without systematics.

with a corresponding sensitivity equal to 6.4 $\rm ps^{-1}$.

When also the fully reconstructed events are included in the fit, taking into account correlated systematic uncertainties, the limit and the sensitivity are better, as expected, and for large values of $\Delta m_{\rm s}$, the impact of those events is clearly visible in Fig.7. By combining the fully reconstructed events with the $\rm D_s^- - \ell$, the limit becomes:

$$\Delta m_{\rm s} > 5.4 \ \rm ps^{-1} \ at \ 95\% \ CL \tag{13}$$

with a corresponding sensitivity equal to 7.4 $\rm ps^{-1}$.

As a check a fit to the $\rm B_s^0$ lifetime has been performed giving $\tau_s = 1.58 \pm 0.11$ ps, consistent with the present world average.

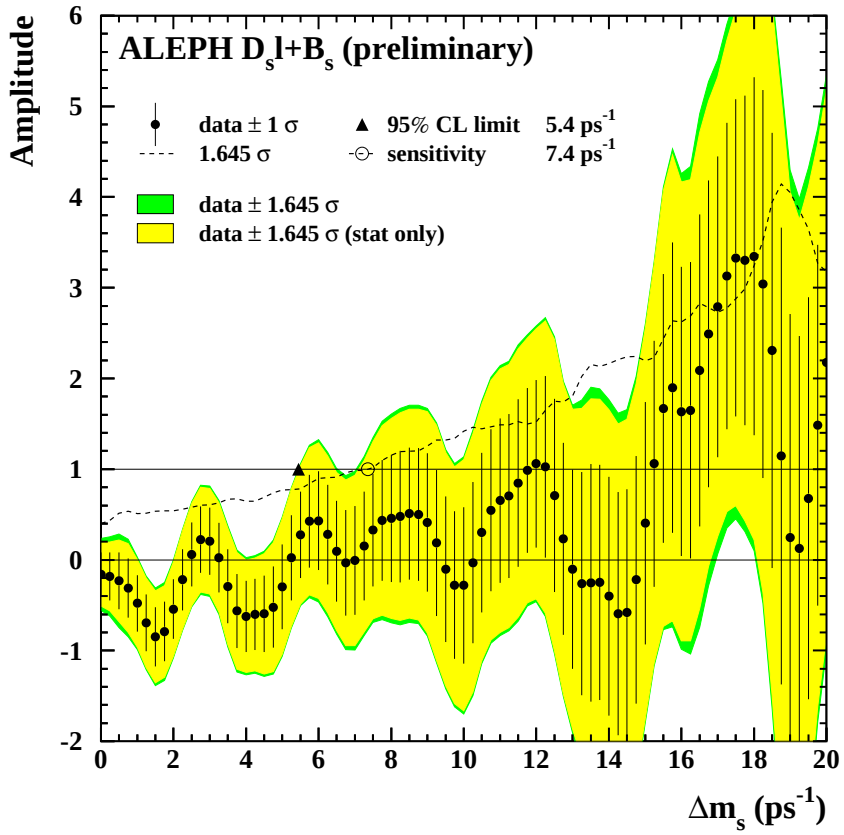

Figure 7: Measured amplitude as a function of Δm_s for the $D_s^- - \ell$ and fully reconstructed events together. The error bars represent the 1σ statistical uncertainties and the shaded bands show the one-sided 95% CL contour, with and without systematics.

6 Conclusions

A lower limit on the oscillation frequency Δm_s of the B_s^0-$\overline{B_s}^0$ system is obtained from recently reprocessed events taken with the ALEPH detector at LEP from 1991 to 1995. Fifty candidates are fully reconstructed in the $D_s^-\pi^+$ and $D_s^- a_1^+$ decay modes in which the D_s^- decays into a $\phi\pi$ and a $K^{*0}K^-$. In addition, leptons are combined with fully reconstructed D_s^- candidates, reconstructed in eight different decay modes, leading to 297 events. The initial state of these B_s^0 has been determined using a neural network algorithm optimized to efficiently use the information of both sides of the event, with an average mistag of about 26%. The limit at 95% confidence level on Δm_s has been determined to be $\Delta m_s > 5.4$ ps^{-1} with an expected sensitivity of 7.4 ps^{-1}. This result superseeds the one in [5].

References

[1] http://www.cern.ch/LEPBOSC/combined_results/summer_1999

[2] H.G. Moser and A. Roussarie, Nucl. Instrum. Meth. **A 384** (1997) 491.

[3] DELPHI Collaboration. *"Study of* B_s^0-$\overline{B_s}^0$ *oscillations using fully reconstructed* B_s^0 *and* D_s^- *events"*, ICHEP'98 contribution.

[4] ALEPH Collaboration, *" Measurement of the* B_s^0 *lifetime and production rate with* $D_s^- - \ell$ *combinations in Z decays"*, Phys. Lett. **B361** (1995) 221.

[5] ALEPH Collaboration, *" Study of the* $B_s^0\overline{B_s}^0$ *oscillation frequency using* $D_s^- - \ell$ *combinations in Z decays"*, Phys. Lett. **B377** (1996) 205.

[6] ALEPH Collaboration, *" Measurement of the* B_s^0 *lifetime"* Phys. Lett. **B322** (1994) 275.

[7] ALEPH Collaboration, *"Heavy quark tagging with leptons in the ALEPH detector"*, Nucl. Instrum. Meth. **A 346** (1994) 461.

[8] C. Caso et al. (Particle Data Group), Eur. Phys. J. **C3** (1998).

[9] ALEPH Collaboration, *"Determination of* $A_{\rm FB}^b$ *using jet charge measurements in Z decays"*, Phys. Lett. **B 426**, 1-2 (1998) 217.

Study of B_s Oscillations with inclusive semileptonic decays

ALEPH Collaboration

Contact Person: Gaëlle Boix (Gaelle.Boix@cern.ch)

Abstract

An improved search for B_s oscillations is performed using the ALEPH LEP1 data sample, recently reprocessed. The analysis is based on the inclusive tagging of semileptonic b hadron decays. Improved vertexing and selection methods yield a sample increased by a factor 2.2 compared to the previous ALEPH publication with the same method, with better resolution. The other key elements of the analysis (charge tagging and enrichment in B_s candidates) are improved as well. Unbinned maximum likelihood amplitude fits are performed to derive a lower limit of $\Delta m_s > 11.1$ ps^{-1} at 95% C.L. with a sensitivity of 11.9 ps^{-1}.

When combined with the other ALEPH analyses, the limit becomes $\Delta m_s > 10.7$ ps^{-1} at 95% C.L. with a sensitivity equal to 13.1 ps^{-1}.

1 Introduction

The determination of the $B_s - \overline{B}_s$ oscillation frequency Δm_s is one of the major issues in the study of flavour dynamics. Up to date, only lower limits have been set. The World combination of analyses currently available gives $\Delta m_s > 14.6$ ps^{-1} at 95% C.L. [1]. Within the framework of the Standard Model, a measurement of the ratio $\Delta m_s/\Delta m_d$ would allow the extraction of the ratio of Cabibbo-Kobayashi-Maskawa quark mixing matrix elements $|V_{ts}/V_{td}|$, which is proportional to one of the sides of the *Unitarity Triangle*.

During 1998 the LEP1 ALEPH data were reprocessed using a refined version of the reconstruction program. The main improvements concern track reconstruction and particle identification.

The analysis presented here is based on an inclusive lepton sample. Compared to the previous ALEPH inclusive lepton analysis [2], the following improvements are made to increase the sensitivity to B_s oscillations.

- **Vertexing.** A new vertexing algorithm has been developed. The decay length resolution is improved for most of the events and allows a looser event selection keeping the average resolution as in the previous analysis. Resolution classes are defined, and the *pull* correction is parametrized class-by-class.

- **Final State Tagging.** The charge of the lepton is used to tag the flavour of the b hadron at decay. A discriminant variable to distinguish direct $b \to \ell$ decays from cascade $b \to c \to \ell$ is built. Cascade decays yield the wrong tag for the b charge at decay time and need to be rejected. A loose cut is applied on the combined discriminating variable, and the probability that the decay be a $b \to \ell$ is estimated event-by-event.

- **Initial State Tagging.** The flavour of the b hadron at production is determined by combining information from both hemispheres. In the hemisphere opposite to the semileptonic decay, variables correlated with the charge of the other b hadron are selected. In the same hemisphere, tracks produced in the fragmentation of the b quark carry information about the flavour of the b hadron at production time. A single discriminating variable is built, and the flavour mistag probability evaluated event-by-event.

- **B_s Enrichment.** Neutral b hadrons can be distinguished using secondary vertex charge variables. The presence of a fragmentation kaon and the kaon content of the b hadron decay distinguish B_s from B_d. A discriminant variable is built and used to get the b species content on an event-by-event basis.

The note is organized as follows. The event selection is described in Section 2. In Section 3 the proper time reconstruction procedure is explained. The initial state tagging method is presented in Section 4. Section 5 is devoted to the B_s enrichment

procedure. In Section 6 systematic checks are discussed and preliminary results are presented.

2 Event Selection

This analysis uses approximately 4 million hadronic Z decays recorded by the ALEPH detector from 1991 to 1995 at centre-of-mass energies close to the Z peak. Three different Monte Carlo samples have been used: ~ 8M $\mathrm{q\overline{q}}$, ~ 5M $\mathrm{b\overline{b}}$ and ~ 1M $\mathrm{B_s} \to \ell$.

As a first step, a mild pre-selection is applied. Events well contained in the vertex detector acceptance are selected requiring $|\cos\theta_{\mathrm{thrust}}| < 0.85$. Leptons[1] are identified as in [3]. Events are kept if they contain at least one such a lepton candidate. If more than one lepton is found in an event, the one with highest transverse momentum with respect to the b jet (p_T) is taken.

The decay length resolution is a major limiting factor for the sensitivity of the analysis. Further selection criteria are based on the quality of the secondary vertex reconstruction.

2.1 Vertexing

The procedure to reconstruct the b decay vertex follows the same steps as in the previous analysis [2]: a set of *c-tracks* is selected based on their kinematical properties and compatibility with an inclusively reconstructed secondary vertex. These tracks are vertexed together to get the *charmed particle* which is then vertexed with the lepton, to obtain the b vertex position.

Several new features have been introduced:

- A new topological vertexing algorithm that combines information from all charged tracks in the hemisphere with a maximum-likelihood fit is used [4]. This algorithm has better resolution on secondary vertices than the one previously used [2], but fails for some events, in particular at small decay length. Therefore, the old algorithm is used when the new one fails.

- A cone-based jet is formed around the lepton candidate [5]. Its direction is used as improved estimator of the b hadron flight direction for events with three jets or more; in the case of two jet events, instead, the thrust direction is taken as the best estimate of the b hadron direction.

- A B track with the direction described above is built. It is forced to pass through the primary vertex and has angular errors parametrized. This track is used in the b vertex fit together with the lepton and the *charmed particle*.

[1] Here, and throughout this paper, we only consider electrons and muons.

- The flight direction of the *charmed particle* is improved adding the momentum of a photon to it.[2] In the ALEPH reconstruction all photons have their momentum calculated as if they were coming from the IP. Here, however, they had to be taken as coming from the *charm vertex* in order to obtain an improvement on the decay length resolution.

Most of the improvement comes from the addition of the *B track* to the final secondary vertex fit. The photon addition is found to be effective only for 10% of the events.

The decay length obtained with this method is projected onto the b direction. A bias correction, as a function of the measured decay length, is applied to obtain the final b decay length. The decay length error provided by the fit is, in general, underestimated: the *pull* distribution, $(l - l_0)/\sigma_l$, has an *r.m.s.* greater than one. The correction is parametrized as a function of the invariant mass of the *charmed particle* and the reconstructed decay length.

Several regions in the phase space are defined (based on the mass of the *charmed particle*, the angle between the lepton and the *charmed particle*, the number of tracks at the charm vertex and the χ^2 of both c and b vertices) in such a way that events inside a class have, on average, a similar resolution as the average resolution for the previous ALEPH analysis.

This vertexing algorithm, together with the lepton selection, is also a good b event selection: just requiring the event being in the above mentioned phase space regions, on $q\overline{q}$ Monte Carlo events, 83% of the selected sample are $b\overline{b}$. However, this analysis needs a higher b hadron purity and a dedicated b tagging is needed.

2.2 Selection of b events

A b tagging variable, N_b, is built combining, with a neural net, inclusive lifetime variables [6] with lepton variables (momentum and transverse momentum with respect to the jet). The distribution of the events passing the vertex selection is displayed in Figure 8.

Events with $N_b < 0$ are rejected. The sample selected has a b hadron purity of 98%, with only a 10% loss in efficiency. For the events surviving the cut, the b purity is estimated event-by-event from the value of N_b.

2.3 Selection of b $\rightarrow \ell$ decays

After the vertex selection and the b tag cut, the b $\rightarrow \ell$ fraction is only 67%. In the previous analysis, a cut on the transverse momentum of the lepton with respect to

[2] A jet around the *charmed particle* is formed and photons are looked for inside it. If more than one photon with momentum higher than 1 GeV is found, the most energetic in a 16° cone around the jet direction, making an invariant mass of less than 1.8 GeV is taken.

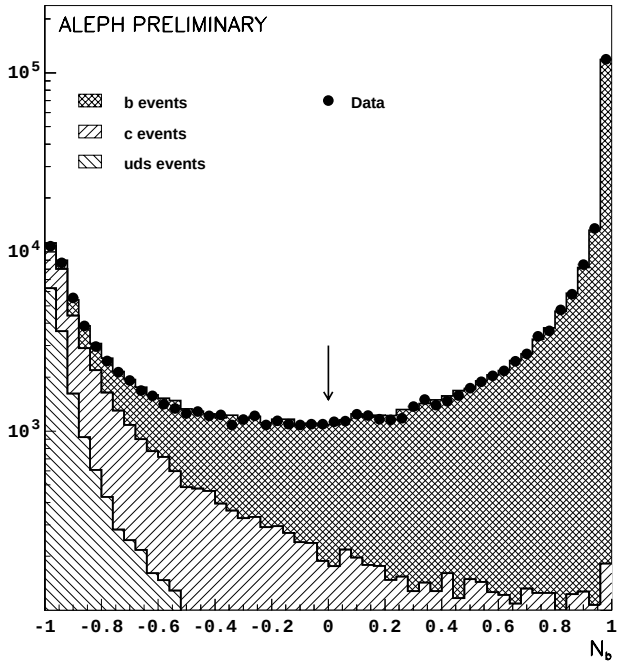

Figure 8: The b tagging variable distribution.

the b jet (p_T) was applied to reject cascade decays ($b \to c \to \ell$). Here, instead, the lepton p_T is combined with other discriminating variables, using a neural net, to get an optimal separation between direct and cascade semileptonic b decays. In addition to the lepton p_T, the variables used are: the lepton momentum, the signed impact parameter significance of the lepton with respect to the charm vertex[3], the neutrino energy[4] and four event topology variables described in [7] (these variables exploit the fact that in the "D+lepton" rest frame, the decay is expected to be spherical for the $b \to c \to \ell$ process and with a high thrust for $b \to \ell$).

The $b \to \ell$ tagging variable, N_{bl}, distribution can be seen in Figure 9. Events with $N_{bl} < -0.5$ are rejected. The position of this cut is optimised to reject those events that have a probability of getting the correct sign from the lepton lower than 0.5.

The final state tag, b hadron flavour at decay, is taken as the sign of the lepton. The mistag probability for each event is parametrized as a function of N_{bl}.

The sample used for the oscillation fit consists of 74026 events in data (to be compared with 33023 in the previous analysis) with a composition evaluated from $q\overline{q}$ events as in Table 5. On average 87.2% of the $b\overline{b}$ events are direct semileptonic decays (to be compared with 93.9% in the previous analysis); however, if only the 50000 events more likely to be $b \to \ell$ are considered, this fraction increases to 94%.

[3] The lepton is expected to be behind the c vertex for $b \to \ell$ decays. The impact parameter sign is given according to the *charmed particle* direction.

[4] See Section 3 for an explanation of its derivation.

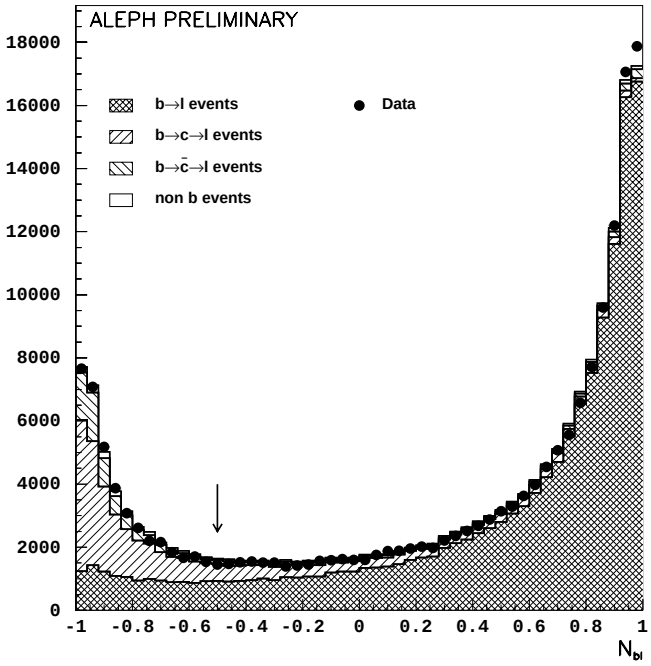

Figure 9: The b $\rightarrow \ell$ tagging variable distribution.

98.6% $b\bar{b}$	1.2% $c\bar{c}$	0.2%uds

Table 5: Final Sample composition

3 Proper Time Reconstruction

The proper time of the b hadron at decay is computed as:

$$t = l m_{\mathrm{B}}/p_{\mathrm{B}},$$

where l is the decay length estimated as explained in Section 2.1, m_{B} is the mass of the b hadron (taken to be 5.3 GeV/c^2), and p_{B} is the estimation of the b hadron momentum performed as follows. The energy of the charmed particle, E_{c}, is estimated as in [2]: a jet is clustered around the charged tracks at the charm vertex until a mass of 2.7 GeV/c^2 is reached, excluding particles with energy less than 0.5 GeV. The energy of the neutrino, E_ν, is estimated applying energy and momentum conservation in the whole event [2]. These two ingredients plus the energy of the lepton candidate, E_ℓ, are used to compute the b momentum as:

$$p_{\mathrm{B}} = \sqrt{(E_{\mathrm{c}} + E_\nu + E_\ell)^2 - {m_{\mathrm{B}}}^2}\,.$$

The error on the proper time is defined as:

$$\sigma_t = \sigma_l m_{\mathrm{B}}/p_{\mathrm{B}} \oplus t\sigma_p, \tag{14}$$

where σ_p is the relative uncertainty on the reconstructed momentum and σ_l is the uncertainty on the measured decay length. Note that the proper time error includes an explicit dependence on the reconstructed proper time t. The decay length error σ_l is obtained event-by-event from the track fit and the primary vertex error with a typical core resolution of 200 μm. The distribution $(p - p_0)/p_0$ is fitted with the sum of two Gaussians in Monte Carlo events to obtain σ_{p_1} and σ_{p_2} and their relative fractions f_{p_1} and f_{p_2} (with $f_{p_2} = 1 - f_{p_1}$); typical values for the relative momentum resolution are $\sim 6\%$ in the core and $\sim 20\%$ for the tails, with $f_{p_1} = 0.55$. The proper time resolution function used in the likelihood fits discussed in Section 6 is written as:

$$Res(t, t_0) \; = \; \sum_{i=1}^{2} f_{p_i} \frac{1}{\sqrt{2\,\pi}\;\sigma_{t_i}} \exp\left[-\frac{1}{2} \left(\frac{t - t_0}{\sigma_{t_i}} \right)^2 \right] . \tag{15}$$

4 Initial State Tag

The flavour state at production time is estimated using two sets of discriminating variables which are combined, with a neural net, into a single tag variable.

For the hemisphere opposite to the semileptonic decay considered, a combined charge estimator is used as in [4].

For the candidate hemisphere, charge estimators are built taking care of not being sensitive to the decay products. The variables used are: **a)** primary vertex charge using all tracks in the b jet[5] weighted according to their probability of coming from the primary vertex[6], **b)** primary vertex charge using all tracks in the b jet except those selected as coming from the charm vertex, **c)** charged fragmentation kaon estimator[7]. Additional variables are used, not discriminant by themselves, but correlated with the tagging power of the above listed. These are: the measured decay length l, the measured momentum $p_{\rm B}$, and $\sigma = \sum_i w_i(1 - w_i)$ which estimates the quality of the track separation. The polar angle of the event thrust axis is also used as a global flavour estimator profiting from the b forward-backward asymmetry.

The distribution of the combined initial state tag variable, $N_{\rm is}$, can be seen on the left side of Figure 10 for the signal $\rm B_s \to \ell$. The effective mistag probability on these events is evaluated to be 24%. On the right of Figure 10 the distribution of the tagging variable is shown for all events.

[5] This b jet is obtained using JADE, with a large y_{cut} of 0.2. This ensures that all tracks from the b hadron decay and the fragmentation tracks closest in phase space are included.

[6] A dedicated neural net has been trained on the selected hemispheres to separate tracks from the primary and secondary vertices. A weight w_i giving the probability to come from the secondary vertex is computed for each track.

[7] A neural net combining kinematical variables and dE/dx is trained to identify fragmentation kaons.

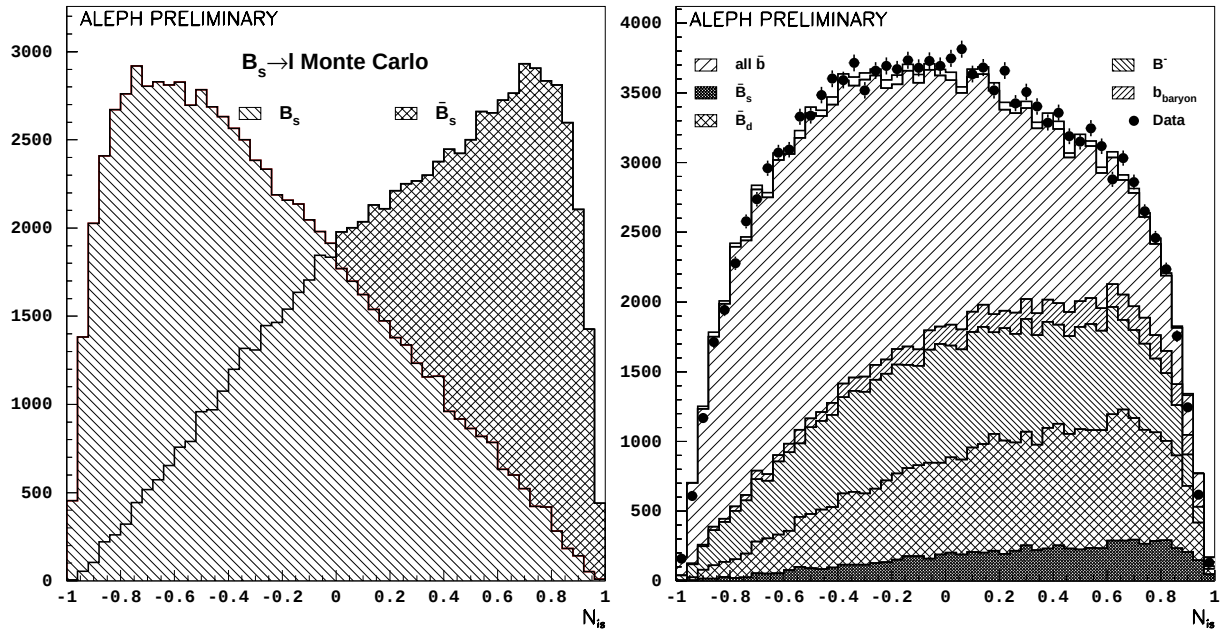

Figure 10: *Left*, Initial state tag variable for Monte Carlo $B_s \to \ell$ events.
Right, Initial state variable for all selected events.

5 Enrichment on B_s decays

In an unbiased b hadron sample only about 10% of the events contain a B_s [8]. The sensitivity of the analysis can be improved by identifying variables which distinguish B_s from other b hadron decays, and evaluating event-by-event the probability for each b hadron species. Variables related to the charge and track multiplicity of the vertex distinguish charged from neutral b hadrons. B_s decays can be separated from the other neutral b hadrons on the basis of the presence of a kaon among the fragmentation tracks. The presence of kaons among the c tracks and their charge correlation with the lepton candidate is a discriminating variable as well.

All discriminating variables are combined, with a neural net, to get a b-species estimator, $N_{\rm enr}$. This estimator is used event-by-event to get the probability for the candidate to be a B_s, B_d, B^+ or b $-$ baryon decay.

A disagreement between data and Monte Carlo is seen the $N_{\rm enr}$ distribution: an excess of data in the B^+ region and a deficit elsewhere. All input charge estimators used to separate neutral from charged b hadrons show the same kind of disagreement, clearly favouring the hypothesis of having more charged b hadrons selected in data than in Monte Carlo. The secondary vertex charge variable has been used to fit the amount of charged and neutral b hadrons that are seen in the data sample selected: 8% more charged b decays are found in data than in Monte Carlo. When the corresponding weights are applied to Monte Carlo events, all the variables that distinguish charged from neutral show a good agreement. The distribution of $N_{\rm enr}$ after this correction

(Fig. 11) still shows some deviation, which is however reduced by more than a factor

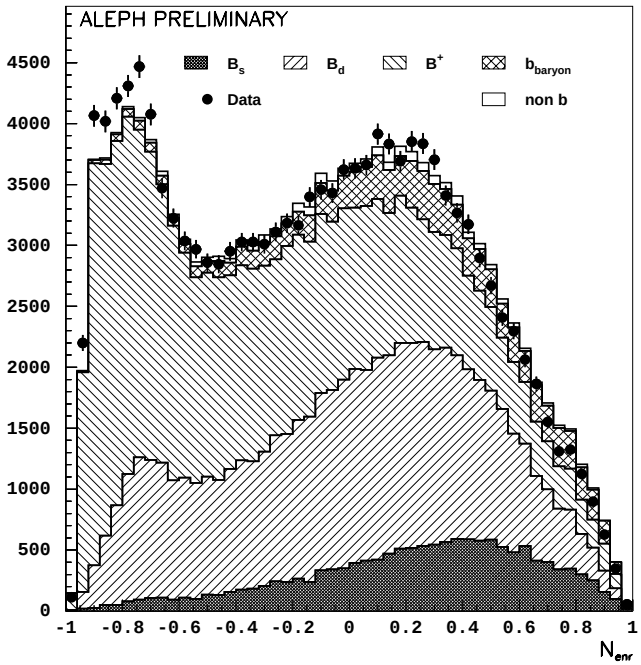

Figure 11: Enrichment variable distribution. B_s decays are concentrated on the right hand side of the plot and B^+ on the left hand side.

of two with respect to the original one. This residual discrepancy is probably due to differences in shape for the variables that distinguish B_s decays from the other neutral b hadrons. The effect of a difference in shape on the event-by-event estimated B_s purity is smaller than the effect of a bias in the selection efficiency. A possible systematic effect due to the residual discrepancy is estimated by removing the weights which re-adjust the charged-to-neutral ratio.

6 The B_s Oscillation fit

A B_s candidate is tagged as unmixed (mixed) when the reconstructed initial and final flavour states are the same (opposite).

The oscillation analysis is performed using the amplitude method [10], which consists of measuring, for each Δm_s value of the oscillation frequency, an amplitude $\mathcal{A}$ and its error $\sigma_{\mathcal{A}}$. The *p.d.f.* used for the signal is therefore:

$$\mathcal{P}_s^{\mathrm{mix,unmix}}(t) \;=\; \frac{1}{2\tau_s}\exp(-t/\tau_s)(1 \mp \mathcal{A}\cos(\Delta m_s t)). \qquad (16)$$

A value of Δm_s can be excluded at 95% C.L. if $\mathcal{A} + 1.645\sigma_{\mathcal{A}} < 1$.

A likelihood function is written for events tagged as mixed and unmixed, taking into account the mistag probability, the b species purities (each b species is described

with its own physical *p.d.f.*, the udsc background is parametrized from Monte Carlo), the proper time resolution and efficiency.

6.1 Systematic Uncertainties

Uncertainties in the evaluation or present knowledge of the input parameters in the fit have been propagated and the corresponding variations in the fitted amplitude have been taken as the systematic error. Table 6 summarizes all systematic uncertainties studied, the statistical error on the amplitude at $\Delta m_{\rm s} = 0, 10, 20$ and 25 ps^{-1} is compared with each of the systematics at the same point.

$\Delta m_{\rm s}$	0 ps^{-1}	10 ps^{-1}	20 ps^{-1}	25 ps^{-1}
$\sigma_{\mathcal{A}}^{stat}$	$\pm$0.081	$\pm$0.466	$\pm$1.430	$\pm$2.477
$f_{\rm s}$	$\pm$0.087	$\pm$0.017	$\pm$0.334	$\pm$0.348
Decay length Resolution	$\pm$0.001	$\pm$0.015	$\pm$0.202	$\pm$0.111
Momentum Resolution	$\pm$0.008	$\pm$0.008	$\pm$0.214	$\pm$0.209
$\tau_{\rm B_s}$	$\pm$0.006	$\pm$0.016	$\pm$0.122	$\pm$0.145
Mistag	$\pm$0.070	$\pm$0.047	$\pm$0.020	$\pm$0.101
$\rm b \to \overline{c} \to \ell$	$\pm$0.065	$\pm$0.046	$\pm$0.023	$\pm$0.103
$\rm b \to \ell / b \to c \to \ell$	$\pm$0.014	$\pm$0.007	$\pm$0.018	$\pm$0.026
Enrichment	$\pm$0.051	$\pm$0.051	$\pm$0.023	$\pm$0.063
Δm_d	$\pm$0.036	$\pm$0.001	$\pm$0.001	$\pm$0.003
Total Systematic	$\pm$0.145	$\pm$0.088	$\pm$0.463	$\pm$0.473

Table 6: Systematic uncertainties on the amplitude at different $\Delta m_{\rm s}$ values compared to the statistical error at the same point.

The most important systematic uncertainty in such an analysis, in particular at high values of $\Delta m_{\rm s}$, comes from $f_{\rm s}$: the fraction of $\rm B_s$ in an unbiased b hadron sample, which at the moment has still a relatively big uncertainty, $f_{\rm s} = (10.7 \pm 1.4)\%$ [8].

A variation of the decay length resolution by $\pm 3\%$ is considered to take into account possible discrepancies on the vertex algorithm performance between data and Monte Carlo. It has been checked that the same results are obtained, on data and Monte Carlo, when using the vertex algorithm for reconstructing the primary vertex on anti-b tagged events.

A variation of $\pm 10\%$ has been taken for the relative momentum resolution.

The input value for the $\rm B_s$ lifetime is taken as $\tau_{\rm B_s} = 1.54 \pm 0.07$ ps [8].

The Initial State tagging variable is, for the $\rm B_s \to \ell$ signal events, perfectly calibrated with slope 1. For systematic studies this slope is varied by 5% [4].

The input $\rm b \to \overline{c} \to \ell$ branching ratio is $\rm Br(b \to \overline{c} \to \ell) = 1.62 \pm 0.44$ [11].

The values of the b $\to \ell$ and b $\to$ c $\to \ell$ branching ratios used are: Br(b $\to \ell$) = $(10.62 \pm 0.17)\%$ and Br(b $\to$ c $\to \ell$) = $(8.07 \pm 0.25)\%$, with a correlation coefficient of -0.37 [11]. The systematic uncertainty quoted is the combination of the two effects taking into account the correlation.

As explained in Section 5, a discrepancy in the enrichment variable distribution between data and Monte Carlo is seen. Weights are applied to Monte Carlo events to increase by 8% the amount of charged b hadrons and match the data selection. These weights are removed for the systematic uncertainty evaluation.

The B_d oscillation frequency input value is $\Delta m_d = 0.464 \pm 0.018$ ps^{-1} [8].

6.2 Limit on Δm_s

An unbinned likelihood fit is performed on the selected sample. The result is shown in Figure 12. A limit at 95% C.L. can be set at $\Delta m_s > 11.1$ ps^{-1}. The sensitivity of

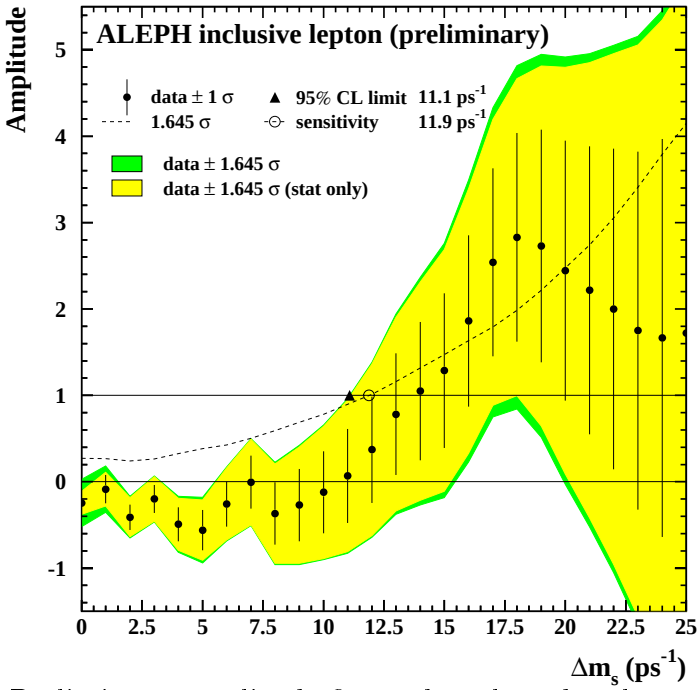

Figure 12: Preliminary amplitude fit on the selected inclusive lepton sample.

the analysis, defined as the test frequency for which amplitude values 0. and 1. can be distinguished at 95% C.L., *i.e.* 1.645 $\sigma_{\mathcal{A}} = 1.$, is equal to 11.9 ps^{-1}. The likelihood curve corresponding to this analysis is given for completeness in Figure 13. There is a minimum around 17.0 ps^{-1} with a depth of 2.

This analysis is combined[8] with previous published and preliminary results from

[8] For the combination with the D_s-l analysis, events in common have been removed from the present sample, and the whole fit repeated.

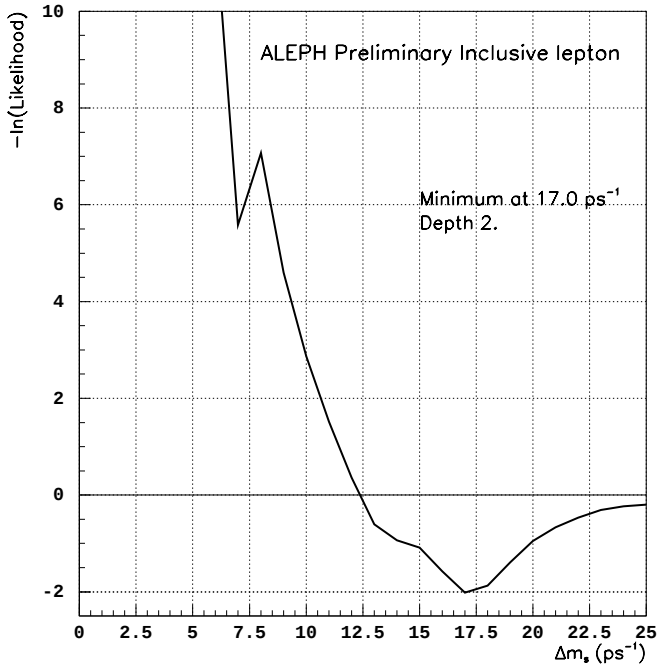

Figure 13: Preliminary log-likelihood curve for the new inclusive lepton analysis.

ALEPH [9, 13], the resulting amplitude plot is shown in Figure 14. The ALEPH combined sensitivity is 13.1 ps^{-1}. The likelihood curve corresponding to the ALEPH combination is shown in Figure 15, with a minimum at 17.3 ps^{-1} with a depth of 3.

7 Conclusion

A lower limit on the oscillation frequency Δm_s of the $B_s - \overline{B}_s$ system is obtained from the recently reprocessed events taken with the ALEPH detector at LEP from 1991 to 1995. From a sample of 74026 semileptonic b hadron decays selected, all values of Δm_s below 11.1 ps^{-1} are excluded at 95% confidence level. The sensitivity of the analysis is determined to be 11.9 ps^{-1}. This analysis supersedes the previous ALEPH inclusive lepton analysis [2].

When combining this analysis with previous ALEPH results [9, 13], the combined limit obtained is $\Delta m_s > 10.7$ ps^{-1} with a sensitivity equal to 13.1 ps^{-1}. The likelihood profile shows a minimum for $\Delta m_s = 17.3$ ps^{-1}, with a significance just over two standard deviations.

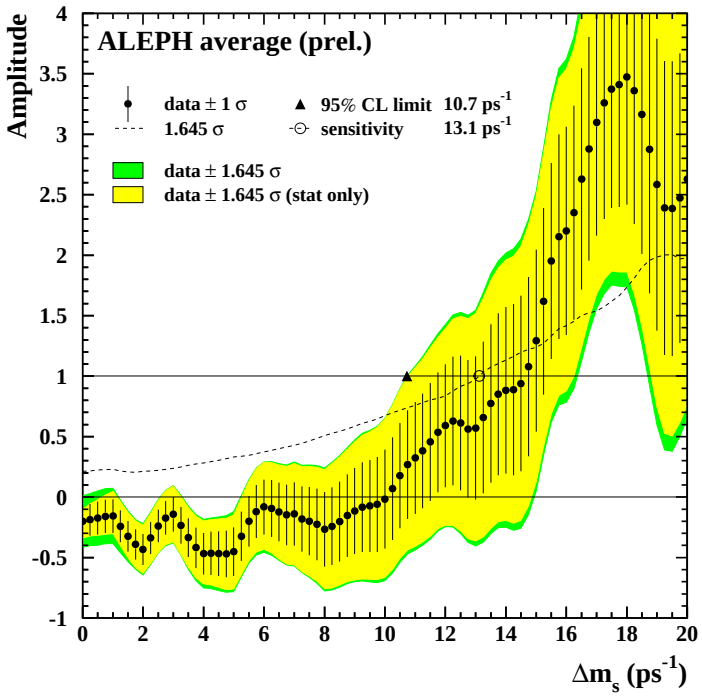

Figure 14: Preliminary ALEPH combined amplitude fit.

References

[1] Averages at the time of 2000 Winter Conferences can be found in `http://www.cern.ch/LEPBOSC/combined_results/moriond_2000/`

[2] The ALEPH Coll., *Euro. Phys. J.* **C7** (1999) 553.

[3] The ALEPH Coll., CERN EP/2000-105, submitted to *Euro. Phys. J.* **C**.

[4] The ALEPH Coll., CONF 2000-045, contribution to ICHEP2000, Osaka.

[5] The OPAL Coll., *Z. Phys.* **C63** (1994) 197.

[6] The ALEPH Coll., *Phys. Lett.* **B401** (1997) 150.

[7] The ALEPH Coll., CONF 99-048, contribution to *HEP99 Tampere*.

[8] The Particle Data Group, *Review of Particle Physics*, *Euro. Phys. J.* **C3** (1998) 1-794 and *Euro. Phys. J.* **C15** (2000) 1-878.

[9] The ALEPH Coll., CONF 2000-024, contribution to *Moriond 2000*.

[10] H.-G. Moser and A. Roussarie, *Nucl. Instrum. and Methods* **A384** (1997) 491.

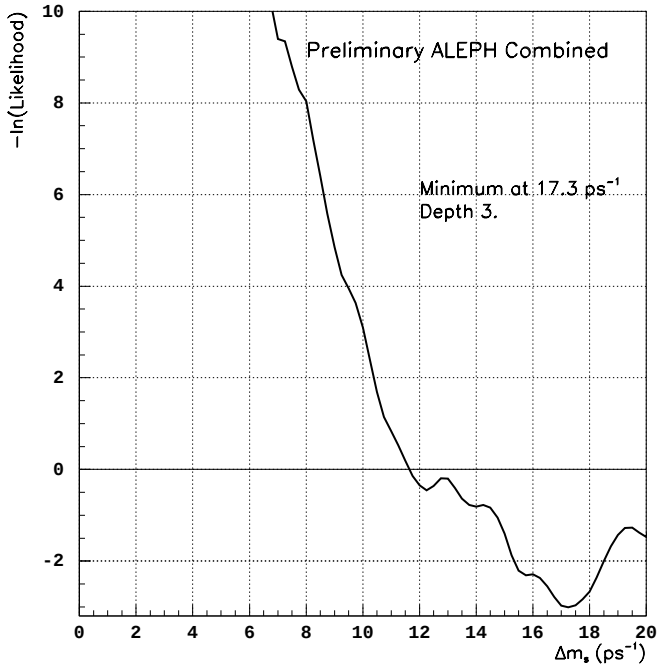

Figure 15: Preliminary log-likelihood curve for the ALEPH combination.

[11] Averages used for the Winter 2000 conference, see
`http://lepewwg.web.cern.ch/LEPEWWG/heavy/`

[12] `http://lepbosc.web.cern.ch/LEPBOSC/references/`

[13] The ALEPH Coll., *Euro. Phys. J.* **C4** (1998) 367.